Vietnam Journal of Mechanics, Vol. 46, No. 3 (2024), pp. 206 – 216
DOI: https://doi.org/10.15625/0866-7136/20934

FREE VIBRATION AND TRANSIENT RESPONSE OF INITIALLY COMPRESSED CNT-REINFORCED COMPOSITE PLATES

Nguyen Van Thinh[1,2], **Nguyen Dong Anh**[3,4], **Le Thi Nhu Trang**[1], **Hoang Van Tung**[5,*]
[1]*Faculty of Civil Engineering, University of Transport Technology, Hanoi, Vietnam*
[2]*Graduate University of Science and Technology, VAST, Hanoi, Vietnam*
[3]*Institute of Mechanics, VAST, Hanoi, Vietnam*
[4]*University of Engineering and Technology, VNU, Hanoi, Vietnam*
[5]*Faculty of Civil Engineering, Hanoi Architectural University, Hanoi, Vietnam*
[*]E-mail: hoangtung0105@gmail.com

Received: 25 February 2024 / Revised: 16 April 2024 / Accepted: 13 June 2024
Published online: 24 September 2024

Abstract. This paper investigates the linear free vibration and nonlinear transient response of carbon nanotube (CNT)-reinforced composite plates subjected to pre-existent compressive load in thermal environments. CNTs are reinforced into matrix according to uniform and functionally graded distributions. The properties of constitutive materials are assumed to be temperature-dependent while the effective properties of nanocomposite are determined using an extended rule of mixture. Governing equations are established within the framework of classical plate theory incorporating von Kármán nonlinearity and initial geometrical imperfection. Analytical solutions of deflection and stress function are assumed to satisfy simply supported boundary conditions, and Galerkin method is applied to obtain a time differential equation including both quadratic and cubic nonlinear terms. Fourth-order Runge–Kutta numerical integration scheme is employed to determine dynamical deflection-time response of nanocomposite plates. Numerical analyses are presented to consider the influences of CNT volume fraction, CNT distribution, initial compressive load, geometrical imperfection, elevated temperature and plate geometry on the natural frequencies and nonlinear dynamical response of nanocomposite plates. The study reveals that the natural frequency and dynamical deflection are strongly decreased and increased when initial compressive load is increased, respectively. Numerical results also find that the natural frequencies are enhanced and dynamical deflection is dropped as a result of increase in volume percentage of CNTs, respectively.

Keywords: CNT-reinforced composite, initial stress, free vibration, nonlinear transient response, geometrical imperfection.

1. INTRODUCTION

Carbon nanotubes (CNTs) possesses unprecedentedly superior properties and are ideal fillers into isotropic matrix to form carbon nanotube reinforced composite (CNTRC), an advanced class of nanocomposite. Stimulated by the concept of functionally graded material (FGM), Shen [1] proposed the functionally graded carbon nanotube reinforced composite (FG-CNTRC) in which CNTs are embedded into matrix according to functional rules in order to obtain desired response of FG-CNTRC structures. Linear static and free vibration analyses of FG-CNTRC plates have been carried out by Liew and coworkers [2–5] using numerical methods and shear deformation plate theories. Linear free vibrations of FG-CNTRC plates without and with piezoelectric layers were investigated in works of Shahrbabaki and Alibeigloo [6] and Kiani [7] employing Ritz method, respectively. Kantorovich-Galerkin and Galerkin methods were employed in works of Wang et al. [8] and Duc et al. [9] studying the linear free vibration of thin FG-CNTRC plates, respectively. Linear free vibrational behavior of simply supported FG-CNTRC rectangular plates was analyzed by Karami et al. [10] and Bouazza and Zenkour [11] utilizing Navier series solutions on the basis of different plate theories. Numerical investigations on the linear free vibration of FG-CNTRC plates with various boundary conditions have been executed by Mehar et al. [12] and Shi [13] making use of finite element method and isogeometric analysis, respectively.

Nonlinear free vibration and dynamical response of FG-CNTRC plates are important and interesting problems. Wang and Shen [14] used higher order shear deformation theory (HSDT) and asymptotic solutions to investigate the nonlinear free vibration of thick FG-CNTRC plates. Tang and Dai [15] employed multi-scale method to study the nonlinear free vibration of simply supported FG-CNTRC plates with hygrothermal effects. Cho [16] used natural element method to analyze the nonlinear free vibration of FG-CNTRC plates with different edge constraints. Nonlinear dynamical response of thick FG-CNTRC plates was presented in the work of Wang and Shen [17] employing HSDT-based perturbation technique. Linear transient analyses of FG-CNTRC plates have been carried out by Lei et al. [18] and Frikha et al. [19] using mesh-free and finite element methods, respectively. Based on isogeometric approach, Phung et al. [20] and Do et al. [21] presented linear dynamic analyses of shear deformable FG-CNTRC plates with various shapes and boundary conditions. There is no investigation on the nonlinear dynamic response of FG-CNTRC plates with initial stresses, to the best of authors' knowledge.

As an extension of previous studies [22–24], the influences of pre-existent compressive load on the nonlinear transient response of FG-CNTRC plates are investigated in this paper using a semi-analytical approach. Basic equations in terms of deflection and stress function are established based on the classical plate theory and solved using analytical

solutions along with the Galerkin method. Fourth-order Runge–Kutta numerical integration scheme is employed to trace nonlinear deflection-time response paths. Parametric studies are carried out and significant remarks are given.

2. STRUCTURAL MODEL AND EFFECTIVE MATERIAL PROPERTIES

Structural model considered in this study is a rectangular plate of length a, width b and thickness h. The plate is located in a Cartesian coordinate system xyz in which the origin is located on the middle surface at a corner, x, y and z axes are the length, width and thickness directions of plate, respectively. The plate is simply supported on all edges and subjected to uniaxial compressive load P acting on two movable edges $x = 0, a$, while two edges $y = 0, b$ are unloaded and tangentially restrained, as illustrated in Fig. 1. The plate is exposed to a thermal environment with uniform temperature rise $\Delta T = T - T_0$ in which T_0 and T are room and elevated temperatures, respectively. The plate is made of carbon nanotube reinforced composite (CNTRC) in which CNTs are straight and aligned in the x direction.

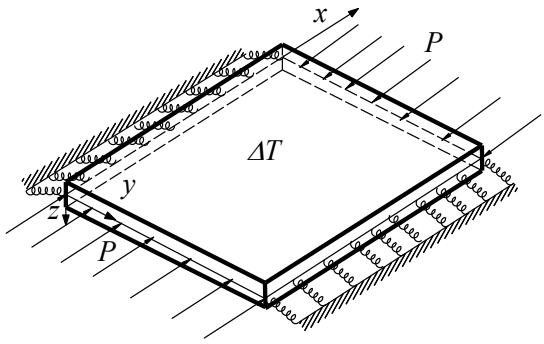

Fig. 1. Structural model and geometries

In this study, CNTs are reinforced into isotropic matrix according to uniform distribution (UD) and functionally graded (FG) distributions named FG-V, FG-Λ, FG-O and FG-X. The volume fraction V_{CNT} of CNTs corresponding to these distributions are determined as [1]

$$V_{CNT}(z) = \begin{cases} V^*_{CNT}, & \text{(UD)} \\ \left(1 + 2\dfrac{z}{h}\right) V^*_{CNT}, & \text{(FG-}\Lambda\text{)} \\ \left(1 - 2\dfrac{z}{h}\right) V^*_{CNT}, & \text{(FG-V)} \\ 2\left(1 - 2\dfrac{|z|}{h}\right) V^*_{CNT}, & \text{(FG-O)} \\ 2\left(2\dfrac{|z|}{h}\right) V^*_{CNT}, & \text{(FG-X)} \end{cases} \tag{1}$$

in which V^*_{CNT} is total volume fraction of CNTs. The effective elastic moduli E_{11} and E_{22} in longitudinal and transverse directions, respectively, and effective shear modulus G_{12}

are estimated using an extended rule of mixture as [1]

$$E_{11} = \eta_1 V_{CNT} E_{11}^{CNT} + V_m E^m, \tag{2a}$$

$$\frac{\eta_2}{E_{22}} = \frac{V_{CNT}}{E_{22}^{CNT}} + \frac{V_m}{E^m}, \tag{2b}$$

$$\frac{\eta_3}{G_{12}} = \frac{V_{CNT}}{G_{12}^{CNT}} + \frac{V_m}{G^m}, \tag{2c}$$

where $V_m = 1 - V_{CNT}$, E^m and G^m are volume fraction, elastic modulus and shear modulus of matrix, respectively, $E_{11}^{CNT}, E_{22}^{CNT}$ and G_{12}^{CNT} are elastic and shear moduli of CNTs, respectively. In the above Eqs. (2), η_1, η_2, η_3 are CNT efficiency parameters taking into account size effect of reinforcements. Effective Poisson ratio ν_{12} is assumed to be constant and determined using conventional rule of mixture as [1]

$$\nu_{12} = V_{CNT}^* \nu_{12}^{CNT} + (1 - V_{CNT}^*)\, \nu^m, \tag{3}$$

where ν_{12}^{CNT} and ν^m are Poisson ratios of CNT and matrix, respectively. Similarly, the effective mass density ρ is estimated as the following [14]

$$\rho = V_{CNT} \rho^{CNT} + V_m \rho^m, \tag{4}$$

where ρ^{CNT} and ρ^m are mass densities of CNT and matrix, respectively. Effective thermal expansion coefficients α_{11} and α_{22} in the longitudinal and transverse directions, respectively, are determined using Schapery model as [14, 17]

$$\alpha_{11} = \frac{V_{CNT} E_{11}^{CNT} \alpha_{11}^{CNT} + V_m E^m \alpha^m}{V_{CNT} E_{11}^{CNT} + V_m E^m}, \tag{5a}$$

$$\alpha_{22} = \left(1 + \nu_{12}^{CNT}\right) V_{CNT} \alpha_{22}^{CNT} + (1 + \nu^m)\, V_m \alpha^m - \nu_{12} \alpha_{11}, \tag{5b}$$

in which $\alpha_{11}^{CNT}, \alpha_{22}^{CNT}$ and α^m are thermal expansion coefficients of CNT and matrix, respectively.

3. FORMULATIONS

In this study, CNTRC plates are assumed to be thin and geometrically imperfect. Classical plate theory (CPT) is used to establish governing equations, namely, motion equation and strain compatibility equation. Motion equation of CNTRC plates is [23]

$$\begin{aligned} I_0 w_{,tt} + a_{11} w_{,xxxx} + a_{21} w_{,yyyy} + a_{31} w_{,xxyy} + a_{41} f_{,xxyy} - f_{,yy} \left(w_{,xx} + w_{,xx}^*\right) \\ + 2 f_{,xy} \left(w_{,xy} + w_{,xy}^*\right) - f_{,xx} \left(w_{,yy} + w_{,yy}^*\right) - q = 0, \end{aligned} \tag{6}$$

in which t is time variable, q is uniform lateral pressure, $f(x,y,t)$ is a stress function and I_0 is mass moment of inertia defined as

$$I_0 = \int_{-h/2}^{h/2} \rho \mathrm{d}z. \tag{7}$$

Furthermore, in the above Eq. (6), $w(x,y,t)$ and $w^*(x,y)$ are deflection and geometrical imperfection functions, respectively, and coefficients $a_{11},\ldots,a_{41}$ can be found in work [25]. Strain compatibility equation of a CNTRC plate is written in the form [25]

$$\begin{aligned} a_{12}f_{,xxxx} + a_{22}f_{,xxyy} + a_{32}f_{,yyyy} + a_{42}w_{,xxxx} + a_{52}w_{,xxyy} + a_{62}w_{,yyyy} - w_{,xy}^2 \\ + w_{,xx}w_{,yy} - 2w_{,xy}w_{,xy}^* + w_{,xx}w_{,yy}^* + w_{,yy}w_{,xx}^* = 0, \end{aligned} \tag{8}$$

where the detailed expressions of coefficients $a_{12},\ldots,a_{62}$ can be found in the work [25].

To satisfy simply supported boundary conditions, analytical solutions are assumed as [23]

$$w(x,y,t) = W(t)\sin\beta_m x \sin\delta_n y, \quad w^*(x,y) = \mu h \sin\beta_m x \sin\delta_n y, \tag{9a}$$

$$\begin{aligned} f(x,y,t) = {} & A_1(t)\cos 2\beta_m x + A_2(t)\cos 2\delta_n y + A_3(t)\sin\beta_m x \sin\delta_n y \\ & + \frac{1}{2}N_{x0}y^2 + \frac{1}{2}N_{y0}x^2, \end{aligned} \tag{9b}$$

where $\beta_m = m\pi/a, \delta_n = n\pi/b$ $(m,n = 1,2,\ldots)$, $W(t)$ is dependent-time amplitude of deflection and μ is size of geometric imperfection. In the Eq. (9b), A_1, A_2, A_3 are dependent-time coefficients to be determined, $N_{x0} = -Ph$ is active compressive force resultant on movable edges $x = 0, a$ and N_{y0} is fictitious compressive force resultant at tangentially restrained edges $y = 0, b$ and related to average end-shortening displacement on these edges as [25]

$$N_{y0} = -\frac{c}{ab}\int_0^a \int_0^b \frac{\partial v}{\partial y}\mathrm{d}y\mathrm{d}x, \tag{10}$$

in which v is in-plane displacement in the y direction of the middle surface and c is average tangential stiffness parameter.

By substituting the solutions (9) into compatibility equation (8), we receive

$$\begin{aligned} A_1 = \frac{\delta_n^2}{32a_{12}\beta_m^2}W\left(W + 2\mu h\right), \quad A_2 = \frac{\beta_m^2}{32a_{32}\delta_n^2}W\left(W + 2\mu h\right), \\ A_3 = -\frac{a_{42}\beta_m^4 + a_{52}\beta_m^2\delta_n^2 + a_{62}\delta_n^4}{a_{12}\beta_m^4 + a_{22}\beta_m^2\delta_n^2 + a_{32}\delta_n^4}W. \end{aligned} \tag{11}$$

By determining N_{y0} from Eq. (10), putting solutions (9) into motion equation (6) and applying Galerkin method, we have

$$I_0 h\frac{d^2\overline{W}}{dt^2} + g_1\overline{W} + g_2\overline{W}\left(\overline{W}+\mu\right) + g_3\overline{W}\left(\overline{W}+\mu\right)\left(\overline{W}+2\mu\right) + \left(g_4\Delta T - g_5 P\right)\left(\overline{W}+\mu\right) = \frac{16q}{mn\pi^2}, \tag{12}$$

where $\overline{W} = W/h$ and $g_1, \ldots, g_5$ are coefficients depending on material and geometry properties and in-plane boundary condition on unloaded edges and not displayed here for the sake of brevity. Eq. (12) represents nonlinear forced vibration of geometrically imperfect CNTRC plates in the thermal environments. When lateral pressure and nonlinear terms are neglected, Eq. (12) leads to the following equation

$$I_0 h\frac{d^2\overline{W}}{dt^2} + \left(g_1 + \mu g_2 + 2\mu^2 g_3 + g_4\Delta T - g_5 P\right)\overline{W} = \left(g_5 P - g_4\Delta T\right)\mu. \tag{13}$$

This equation describes the linear free vibration of geometrically imperfect CNTRC plates undergoing pre-existent compressive load in thermal environments. Natural frequencies are determined as

$$\omega_L = \sqrt{\frac{g_1 + \mu g_2 + 2\mu^2 g_3 + g_4\Delta T - g_5 P}{I_0 h}}. \tag{14}$$

In numerical results, non-dimensional natural frequencies are computed as

$$\omega_L^* = \omega_L \frac{a^2}{h}\sqrt{\frac{\rho^m}{E_0^m}}, \tag{15}$$

in which E_0^m is value of E^m calculated at room temperature $T_0 = 300$ K.

4. NUMERICAL RESULTS AND DISCUSSION

This section presents numerical results for dynamical analyses of CNTRC plates made of Poly (methyl methacrylate), referred to as PMMA, as matrix and (10, 10) single walled carbon nanotubes (SWCNTs) as reinforcements. The material properties of the PMMA are $\rho^m = 1150\text{kg/m}^3$, $\nu^m = 0.34$, $\alpha_m = 45\left(1 + 0.0005\Delta T\right) \times 10^{-6}/\text{K}$ and $E^m = (3.52 - 0.0034T)$ GPa, in which $T = T_0 + \Delta T$ and $T_0 = 300$ K [14]. The Poisson's ratio and mass density of (10, 10) SWCNTs are $\nu_{12}^{CNT} = 0.175$, $\rho^{CNT} = 1400$ kg/m^3 [14]. The material properties E_{11}^{CNT}, E_{22}^{CNT}, G_{12}^{CNT}, α_{11}^{CNT}, α_{22}^{CNT} of (10, 10) SWCNT have been given in many previous works, e.g. [1, 14, 17], and are not displayed here for the sake of brevity. Moreover, the CNT efficiency parameters η_1, η_2, η_3 corresponding to values of $V_{CNT}^* = 0.12, 0.17, 0.28$ are the same as those reported in works [14, 17].

As part of verification, the non-dimensional fundamental natural frequencies of square FG-CNTRC plates with movable edges and without initial compressive loads are computed employing Eq. (15) and given in Table 1 in comparison with results reported in the work of Cho [16] using natural element method and FSDT. As can be seen, a good agreement is achieved in this comparison.

Table 1. Comparison of non-dimensional fundamental natural frequencies ω_L^* of square FG-CNTRC plates with movable edges ($b/h = 100$, $V_{CNT}^* = 0.28$, $T = 300$ K)

Reference	UD	FG-V	FG-O	FG-X
Cho [16]	26.5782	22.0928	19.4445	32.1978
Present	26.5562	21.9514	19.0434	32.4063

The effects of CNT distribution, initial compressive stress P and thermal environments on the dimensionless fundamental natural frequencies ω_L^* of square CNTRC plates with movable edges are shown in Table 2 in which P_{cr} is critical buckling compressive load. It is recognized that the frequencies are significantly and slightly reduced when compressive load P and temperature T are increased, respectively. Among five types of CNT distribution, FG-O and FG-X plates have the smallest and largest frequencies, while uniform distribution (UD) brings to an intermediate frequency of CNTRC plate.

Table 2. Non-dimensional fundamental natural frequencies ω_L^* of square FG-CNTRC plates with movable edges ($b/h = 40$, $V_{CNT}^* = 0.17$)

T (K)	P/P_{cr}	UD	FG-V	FG-Λ	FG-O	FG-X
300	0	21.1948	17.6118	17.6118	15.3339	25.7656
	0.3	17.7329	14.7351	14.7351	12.8293	21.5570
	0.6	13.4048	11.1387	11.1387	9.6980	16.2956
	0.9	6.7024	5.5693	5.5693	4.8490	8.1478
400	0	20.9895	17.4055	17.4055	15.1449	25.5388
	0.3	17.5611	14.5625	14.5625	12.6711	21.3673
	0.6	13.2749	11.0082	11.0082	9.5785	16.1521
	0.9	6.6375	5.5041	5.5041	4.7892	8.0761

Fig. 2 considers the effects of initial compressive load P and CNT volume fraction V_{CNT}^* on the natural frequencies of FG-X plates. It is evident that the natural frequencies are substantially reduced and enhanced when P and V_{CNT}^* are increased, respectively. It is also realized that the frequencies are zero-valued when P reaches critical buckling value.

The nonlinear transient response of square CNTRC plates with fundamental shape mode $(m, n) = (1, 1)$, geometry properties $a/b = 1$, $h = 2$ mm subjected to suddenly

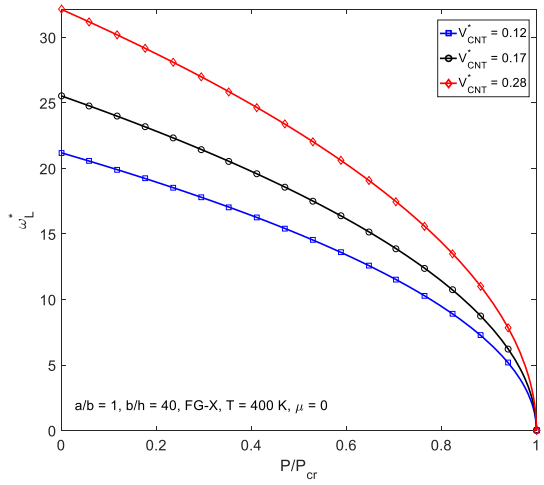

Fig. 2. Effects of pre-existent compressive load and CNT volume fraction on the natural frequencies of FG-X plates

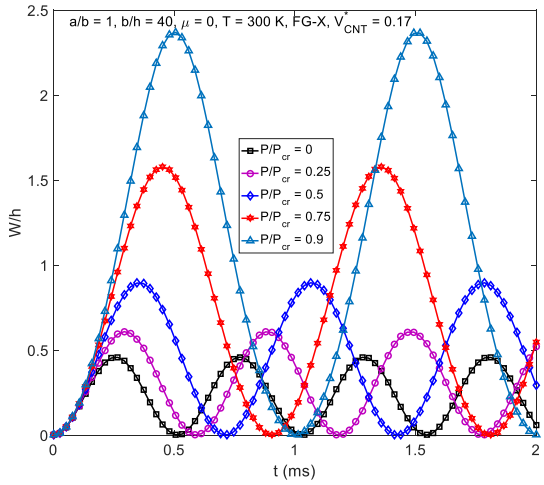

Fig. 3. Effects of initial compressive load on nonlinear transient response of FG-X plates with immovable unloaded edges

applied uniform load $q = 10^5$ N/m^2 is presented in the remainder of this section. Fig. 3 indicates that amplitude of dynamical deflection and vibration period are significantly increased when initial compressive load is increased. Next, Fig. 4 demonstrates that increase in the volume percentage of CNTs leads to pronounced decreases in both vibration amplitude and period.

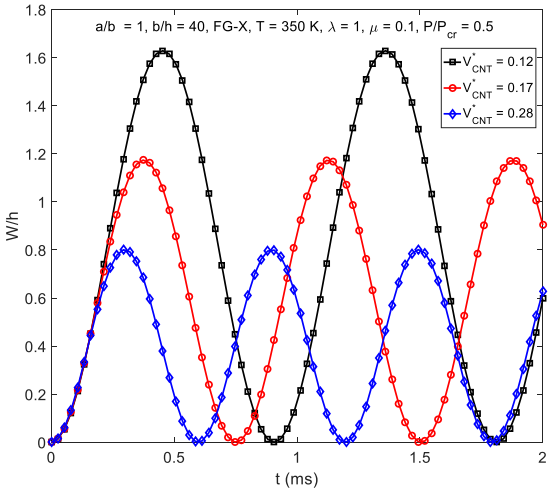

Fig. 4. Effects of CNT volume fraction on nonlinear transient response of FG-X plates with immovable unloaded edges

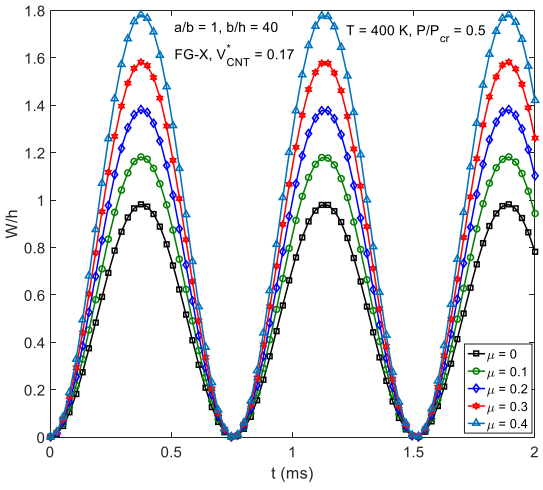

Fig. 5. Effects of geometrical imperfection on nonlinear transient response of FG-X plates with immovable unloaded edges

Finally, Fig. 5 shows that amplitude of dynamical deflection is considerably increased as the size of geometric imperfection is larger. It is also observed that geometrical imperfection slightly affects the vibration period of initially compressed CNTRC plates.

5. CONCLUDING REMARKS

The influences of initial compressive stress on the free vibration and transient response of geometrically imperfect CNTRC plates in thermal environments have been investigated. From the obtained results, the following remarks are reached:

- Natural frequencies and amplitude of dynamical deflection of CNTRC plates are significantly decreased and increased when initial compressive load is increased, respectively.

- Natural frequencies and amplitude of dynamical deflection of CNTRC plates are remarkably enhanced and dropped as a result of increase in volume percentage of CNTs, respectively.

- Initial geometric imperfection strongly affects the nonlinear transient response of initially stressed CNTRC plates and the amplitude of dynamical deflection is considerably enhanced due to the enhancement of imperfection size. Meanwhile, initial geometrical imperfection has marginal influences on the vibration frequencies of initially compressed CNTRC plates.

DECLARATION OF COMPETING INTEREST

The authors declare that they have no known competing financial interests or personal relationships that could have appeared to influence the work reported in this paper.

ACKNOWLEDGEMENT

This research is funded by Vietnam National Foundation for Science and Technology Development (NAFOSTED) under grant number 107.02-2023.26.

REFERENCES

[1] H.-S. Shen. Nonlinear bending of functionally graded carbon nanotube-reinforced composite plates in thermal environments. *Composite Structures*, **91**, (2009), pp. 9–19. https://doi.org/10.1016/j.compstruct.2009.04.026.

[2] P. Zhu, Z. X. Lei, and K. M. Liew. Static and free vibration analyses of carbon nanotube-reinforced composite plates using finite element method with first order shear deformation plate theory. *Composite Structures*, **94**, (2012), pp. 1450–1460. https://doi.org/10.1016/j.compstruct.2011.11.010.

[3] Z. X. Lei, K. M. Liew, and J. L. Yu. Free vibration analysis of functionally graded carbon nanotube-reinforced composite plates using the element-free kp-Ritz method in thermal environment. *Composite Structures*, **106**, (2013), pp. 128–138. https://doi.org/10.1016/j.compstruct.2013.06.003.

[4] B. A. Selim, L. W. Zhang, and K. M. Liew. Vibration analysis of CNT reinforced functionally graded composite plates in a thermal environment based on Reddy's higher-order shear deformation theory. *Composite Structures*, **156**, (2016), pp. 276–290. https://doi.org/10.1016/j.compstruct.2015.10.026.

[5] L. W. Zhang, W. C. Cui, and K. M. Liew. Vibration analysis of functionally graded carbon nanotube reinforced composite thick plates with elastically restrained edges. *International Journal of Mechanical Sciences*, **103**, (2015), pp. 9–21. https://doi.org/10.1016/j.ijmecsci.2015.08.021.

[6] E. Abdollahzadeh Shahrbabaki and A. Alibeigloo. Three-dimensional free vibration of carbon nanotube-reinforced composite plates with various boundary conditions using Ritz method. *Composite Structures*, **111**, (2014), pp. 362–370. https://doi.org/10.1016/j.compstruct.2014.01.013.

[7] Y. Kiani. Free vibration of functionally graded carbon nanotube reinforced composite plates integrated with piezoelectric layers. *Computers & Mathematics with Applications*, **72**, (2016), pp. 2433–2449. https://doi.org/10.1016/j.camwa.2016.09.007.

[8] M. Wang, Z.-M. Li, and P. Qiao. Semi-analytical solutions to buckling and free vibration analysis of carbon nanotube-reinforced composite thin plates. *Composite Structures*, **144**, (2016), pp. 33–43. https://doi.org/10.1016/j.compstruct.2016.02.025.

[9] N. D. Duc, J. Lee, T. Nguyen-Thoi, and P. T. Thang. Static response and free vibration of functionally graded carbon nanotube-reinforced composite rectangular plates resting on Winkler–Pasternak elastic foundations. *Aerospace Science and Technology*, **68**, (2017), pp. 391–402. https://doi.org/10.1016/j.ast.2017.05.032.

[10] B. Karami, D. Shahsavari, and M. Janghorban. A comprehensive analytical study on functionally graded carbon nanotube-reinforced composite plates. *Aerospace Science and Technology*, **82–83**, (2018), pp. 499–512. https://doi.org/10.1016/j.ast.2018.10.001.

[11] M. Bouazza and A. M. Zenkour. Vibration of carbon nanotube-reinforced plates via refined nth-higher-order theory. *Archive of Applied Mechanics*, **90**, (2020), pp. 1755–1769. https://doi.org/10.1007/s00419-020-01694-3.

[12] K. Mehar, S. K. Panda, A. Dehengia, and V. R. Kar. Vibration analysis of functionally graded carbon nanotube reinforced composite plate in thermal environment. *Journal of Sandwich Structures & Materials*, **18**, (2015), pp. 151–173. https://doi.org/10.1177/1099636215613324.

[13] P. Shi. Three-dimensional isogeometric analysis of functionally graded carbon nanotube-reinforced composite plates. *Archive of Applied Mechanics*, **92**, (2022), pp. 3033–3063. https://doi.org/10.1007/s00419-022-02224-z.

[14] Z.-X. Wang and H.-S. Shen. Nonlinear vibration of nanotube-reinforced composite plates in thermal environments. *Computational Materials Science*, **50**, (2011), pp. 2319–2330. https://doi.org/10.1016/j.commatsci.2011.03.005.

[15] H. Tang and H.-L. Dai. Nonlinear vibration behavior of CNTRC plate with different distribution of CNTs under hygrothermal effects. *Aerospace Science and Technology*, **115**, (2021). https://doi.org/10.1016/j.ast.2021.106767.

[16] J. R. Cho. Nonlinear free vibration of functionally graded CNT-reinforced composite plates. *Composite Structures*, **281**, (2022). https://doi.org/10.1016/j.compstruct.2021.115101.

[17] Z.-X. Wang and H.-S. Shen. Nonlinear dynamic response of nanotube-reinforced composite plates resting on elastic foundations in thermal environments. *Nonlinear Dynamics*, **70**, (2012), pp. 735–754. https://doi.org/10.1007/s11071-012-0491-2.

[18] Z. X. Lei, L. W. Zhang, and K. M. Liew. Elastodynamic analysis of carbon nanotube-reinforced functionally graded plates. *International Journal of Mechanical Sciences*, **99**, (2015), pp. 208–217. https://doi.org/10.1016/j.ijmecsci.2015.05.014.

[19] A. Frikha, S. Zghal, and F. Dammak. Dynamic analysis of functionally graded carbon nanotubes-reinforced plate and shell structures using a double directors finite shell element. *Aerospace Science and Technology*, **78**, (2018), pp. 438–451. https://doi.org/10.1016/j.ast.2018.04.048.

[20] P. Phung-Van, M. Abdel-Wahab, K. M. Liew, S. P. A. Bordas, and H. Nguyen-Xuan. Isogeometric analysis of functionally graded carbon nanotube-reinforced composite plates using higher-order shear deformation theory. *Composite Structures*, **123**, (2015), pp. 137–149. https://doi.org/10.1016/j.compstruct.2014.12.021.

[21] V. N. Van Do, J.-T. Jeon, and C.-H. Lee. Dynamic analysis of carbon nanotube reinforced composite plates by using Bézier extraction based isogeometric finite element combined with higher-order shear deformation theory. *Mechanics of Materials*, **142**, (2020). https://doi.org/10.1016/j.mechmat.2019.103307.

[22] L. T. Nhu Trang and H. Van Tung. Tangential edge constraint sensitivity of nonlinear stability of CNT-reinforced composite plates under compressive and thermomechanical loadings. *Journal of Engineering Mechanics*, **144**, (2018). https://doi.org/10.1061/(asce)em.1943-7889.0001479.

[23] N. D. Anh, N. V. Thinh, and H. V. Tung. Thermoelastic nonlinear vibration and dynamical response of geometrically imperfect carbon nanotube-reinforced composite plates on elastic foundations including tangential edge constraints. *Journal of Thermoplastic Composite Materials*, **37**, (2023), pp. 1067–1093. https://doi.org/10.1177/08927057231191454.

[24] N. D. Anh, N. Van Thinh, and H. Van Tung. Nonlinear thermomechanical vibration of initially stressed functionally graded plates with porosities. *ZAMM - Journal of Applied Mathematics and Mechanics / Zeitschrift für Angewandte Mathematik und Mechanik*, **104**, (2023). https://doi.org/10.1002/zamm.202300528.

[25] H. V. Tung. Thermal buckling and postbuckling behavior of functionally graded carbon-nanotube-reinforced composite plates resting on elastic foundations with tangential-edge restraints. *Journal of Thermal Stresses*, **40**, (2016), pp. 641–663. https://doi.org/10.1080/01495739.2016.1254577.